Rqc2p and 60S ribosomal subunits mediate mRNA-independent elongation of nascent chains

Peter S. Shen,[1] Joseph Park,[2] Yidan Qin,[8,9] Xueming Li,[7]* Krishna Parsawar,[10] Matthew H. Larson,[3,4,5,6] James Cox,[1,10] Yifan Cheng,[7] Alan M. Lambowitz,[8,9] Jonathan S. Weissman,[3,4,5,6]† Onn Brandman,[2]† Adam Frost[1,7]†

In Eukarya, stalled translation induces 40S dissociation and recruitment of the ribosome quality control complex (RQC) to the 60S subunit, which mediates nascent chain degradation. Here we report cryo–electron microscopy structures revealing that the RQC components Rqc2p (YPL009C/Tae2) and Ltn1p (YMR247C/Rkr1) bind to the 60S subunit at sites exposed after 40S dissociation, placing the Ltn1p RING (Really Interesting New Gene) domain near the exit channel and Rqc2p over the P-site transfer RNA (tRNA). We further demonstrate that Rqc2p recruits alanine- and threonine-charged tRNA to the A site and directs the elongation of nascent chains independently of mRNA or 40S subunits. Our work uncovers an unexpected mechanism of protein synthesis, in which a protein—not an mRNA—determines tRNA recruitment and the tagging of nascent chains with carboxy-terminal Ala and Thr extensions ("CAT tails").

[1]Department of Biochemistry, University of Utah, UT 84112, USA. [2]Department of Biochemistry, Stanford University, Palo Alto, CA 94305, USA. [3]Department of Cellular and Molecular Pharmacology, University of California, San Francisco, San Francisco, CA 94158, USA. [4]Howard Hughes Medical Institute, University of California, San Francisco, San Francisco, CA 94158, USA. [5]California Institute for Quantitative Biomedical Research, University of California, San Francisco, San Francisco, CA 94158, USA. [6]Center for RNA Systems Biology, University of California, San Francisco, San Francisco, CA 94158, USA. [7]Department of Biochemistry and Biophysics, University of California, San Francisco, San Francisco, CA 94158, USA. [8]Institute for Cellular and Molecular Biology, University of Texas at Austin, Austin, TX 78712, USA. [9]Department of Molecular Biosciences, University of Texas at Austin, Austin, TX 78712, USA. [10]Mass Spectrometry and Proteomics Core Facility, University of Utah, UT 84112, USA.
*Present address: School of Life Sciences, Tsinghua University, Beijing 100084, China. †Corresponding author. E-mail: jonathan.weissman@ucsf.edu (J.S.W.), onn@stanford.edu (O.B.), adam.frost@ucsf.edu (A.F.)

ACKNOWLEDGMENTS

Electron microscopy was performed at the University of Utah and the University of California. We thank D. Belnap (University of Utah) and M. Braunfeld (University of California, San Francisco) for supervision of the electron microscopes; A. Orendt and the Utah Center for High Performance Computing and the NSF Extreme Science and Engineering Discovery Environment consortium for computational support; D. Sidote (University of Texas at Austin) for help processing RNA-seq data; and D. Herschlag and P. Harbury for helpful comments. Amino acid analysis was performed by J. Shulze at the University of California, Davis Proteomics Core. Edman sequencing was performed at Stanford University's Protein and Nucleic Acid Facility by D. Winant. This work was supported by the Searle Scholars Program (A.F.); Stanford University (O.B.); NIH grants 1DP2GM110772-01 (A.F.), GM37949, and GM37951 (A.M.L.); the Center for RNA Systems Biology grants P50 GM102706 (J.S.W.) and U01 GM098254 (J.S.W.); and the Howard Hughes Medical Institute (J.S.W.). The authors declare no competing financial interests. The cryo-EM structures have been deposited at the Electron Microscopy Data Bank (accession codes 2811, 2812, 6169, 6170, 6171, 6172, 6176, and 6201).

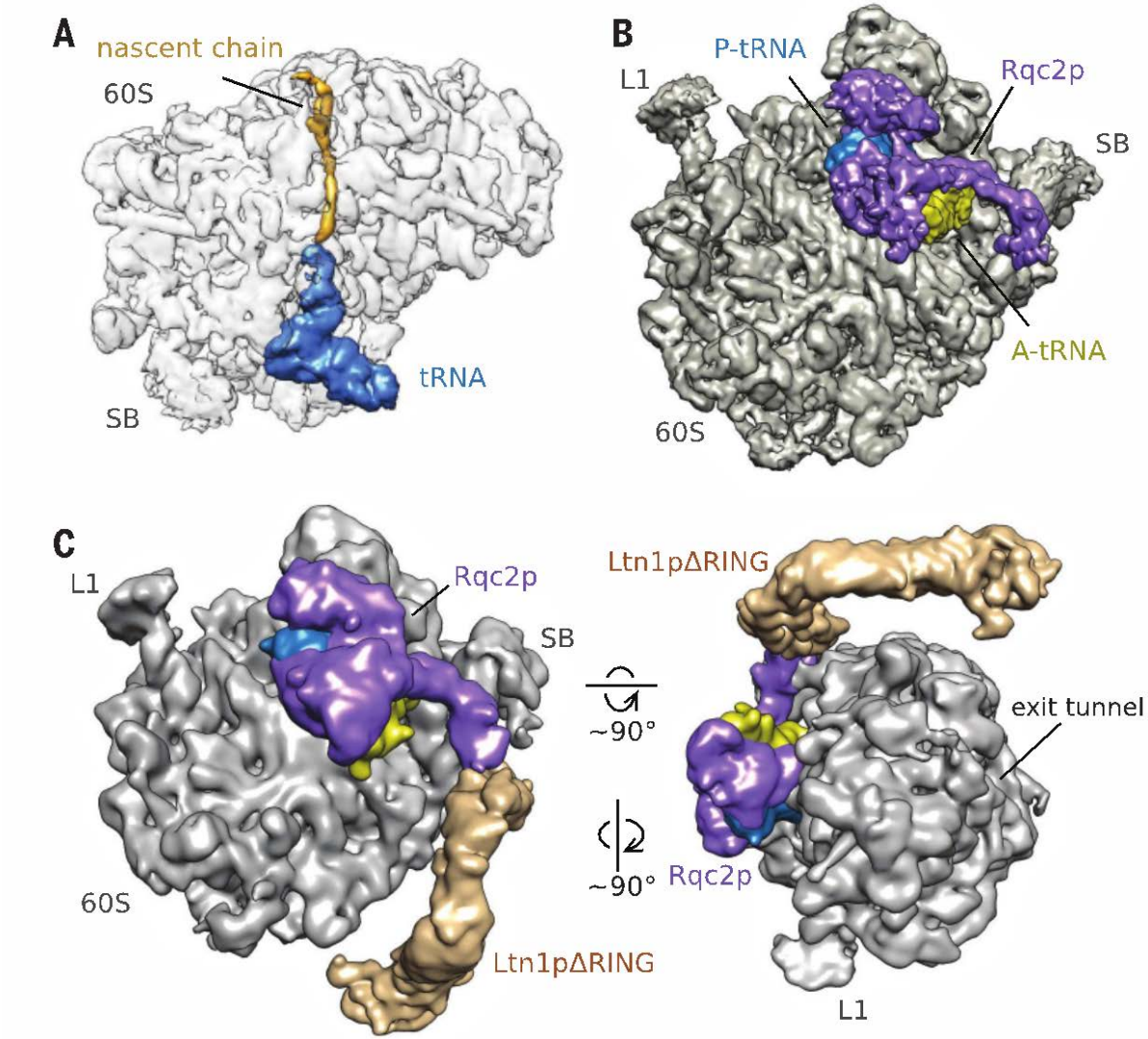

Fig. 1. Cryo-EM reconstructions of peptidyl-tRNA-60S ribosomes bound by the RQC components Rqc2p and Ltn1p. (A) A peptidyl-tRNA-60S complex isolated by immunoprecipitation of Rqc1p. The ribosome density is transparent to visualize the nascent chain. (B) Rqc2p (purple) and an ~A-site tRNA (yellow) bound to peptidyl-tRNA-60S complexes. Landmarks are indicated (L1, L1 stalk; SB, P-stalk base). (C) Ltn1p (tan) bound to Rqc2p-peptidyl-tRNA-60S complexes (B).

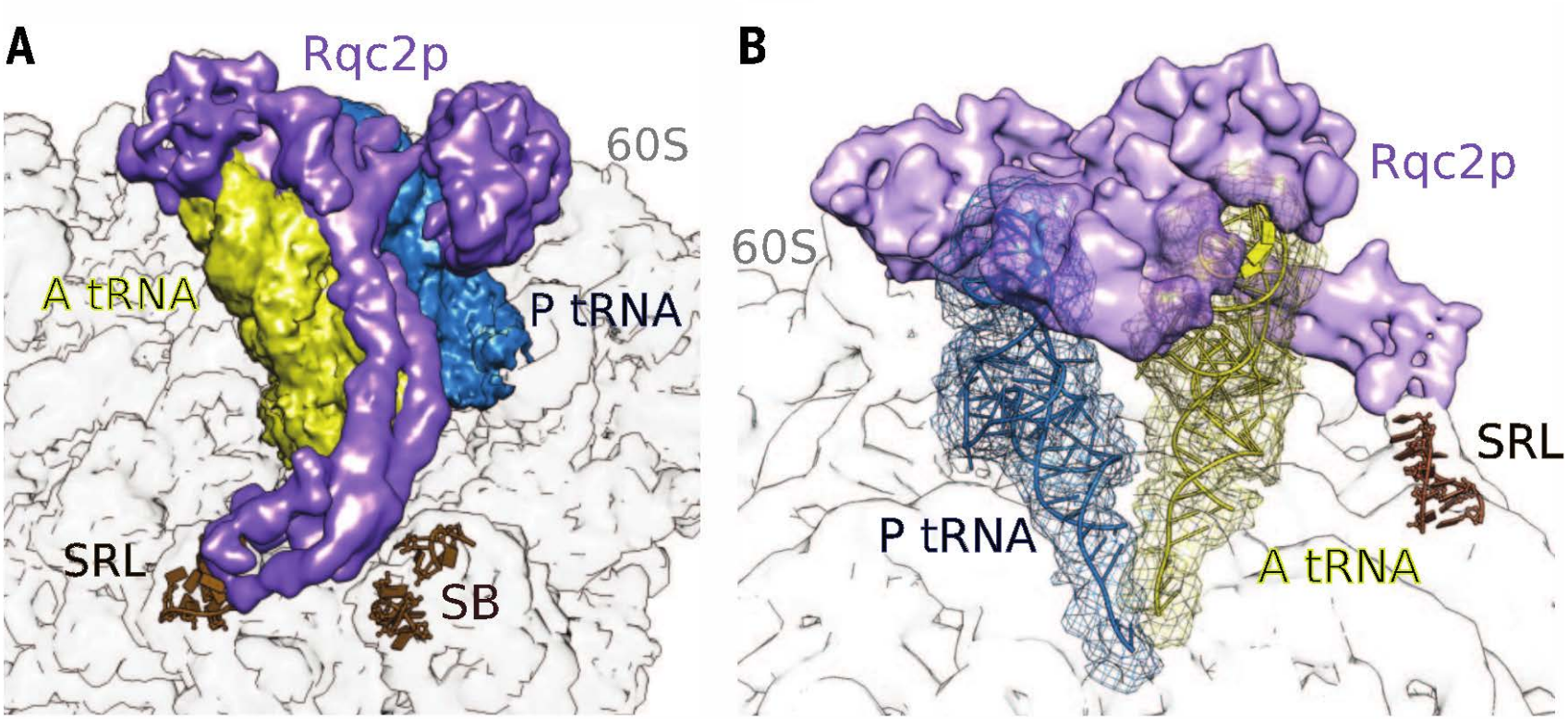

Fig. 2. Rqc2p binding to the 60S ribosome and ~P-site, and ~A-site tRNAs. (A) Rqc2p contacts ~P- and ~A-site tRNAs, the SRL, and P-stalk base ribosomal RNA (SB). (B) Rigid body fitting of tRNAs structures (ribbons) into EM densities (mesh).

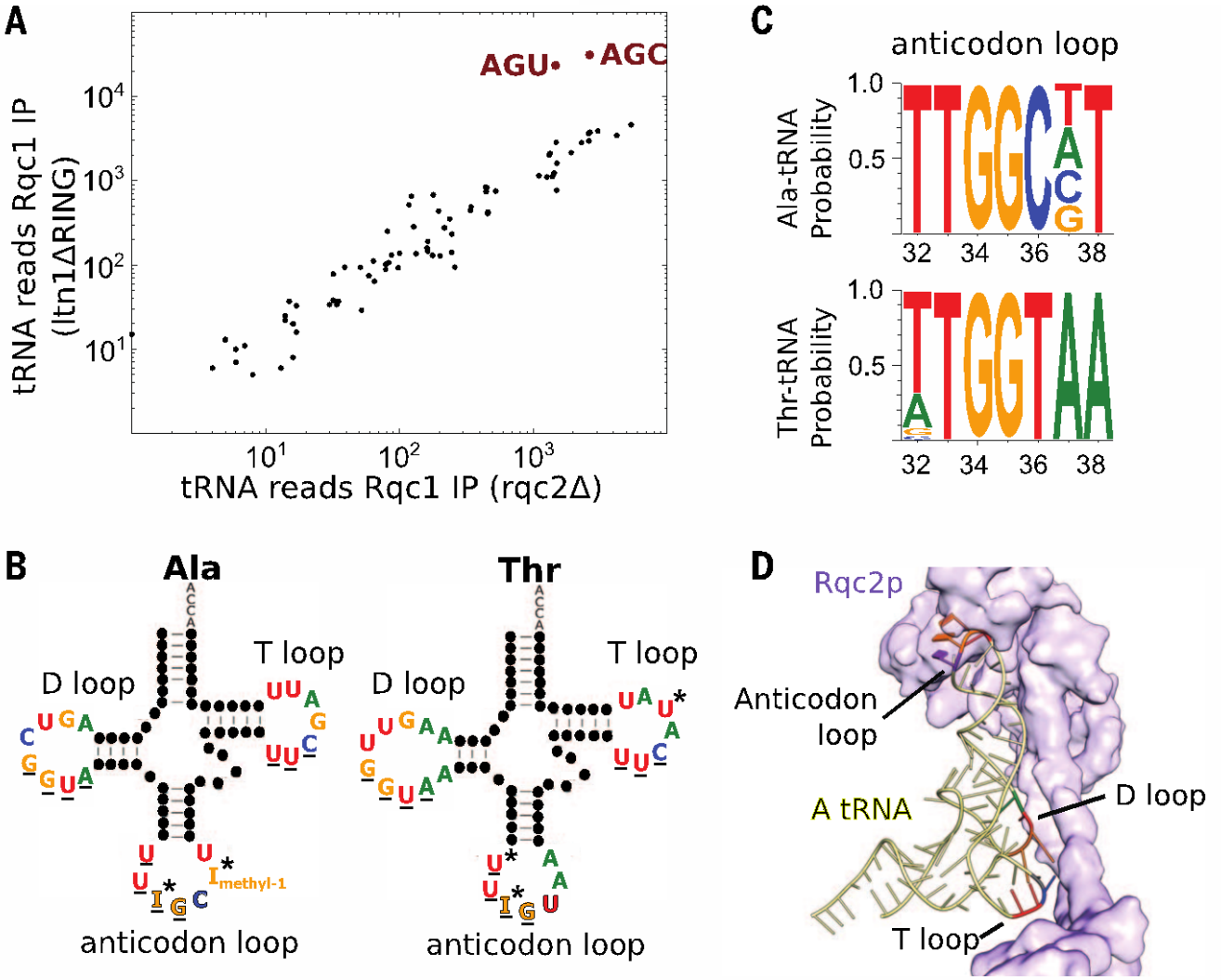

Fig. 3. Rqc2p-dependent enrichment of $tRNA^{Ala(IGC)}$ and $tRNA^{Thr(IGU)}$. (A) tRNA cDNA reads extracted from purified RQC particles and summed per unique anticodon, with versus without Rqc2p. (B) Secondary structures of $tRNA^{Ala(IGC)}$ and $tRNA^{Thr(IGU)}$. Identical nucleotides are underlined. Edited nucleotides are indicated with asterisks (24, 25). (C) Weblogo representation of cDNA sequencing reads related to shared sequences found in anticodon loops (positions 32 to 38) of mature $tRNA^{Ala(IGC)}$ and $tRNA^{Thr(IGU)}$ (26). (D) ~A-tRNA contacts with Rqc2p at the D-, T-, and anticodon loops. Identical nucleotides between $tRNA^{Ala(IGC)}$ and $tRNA^{Thr(IGU)}$ are colored as in (B) (A, green; U, red; C, blue; G, orange) and pyrimidine, purple. Anticodon nucleotides are indicated as slabs.

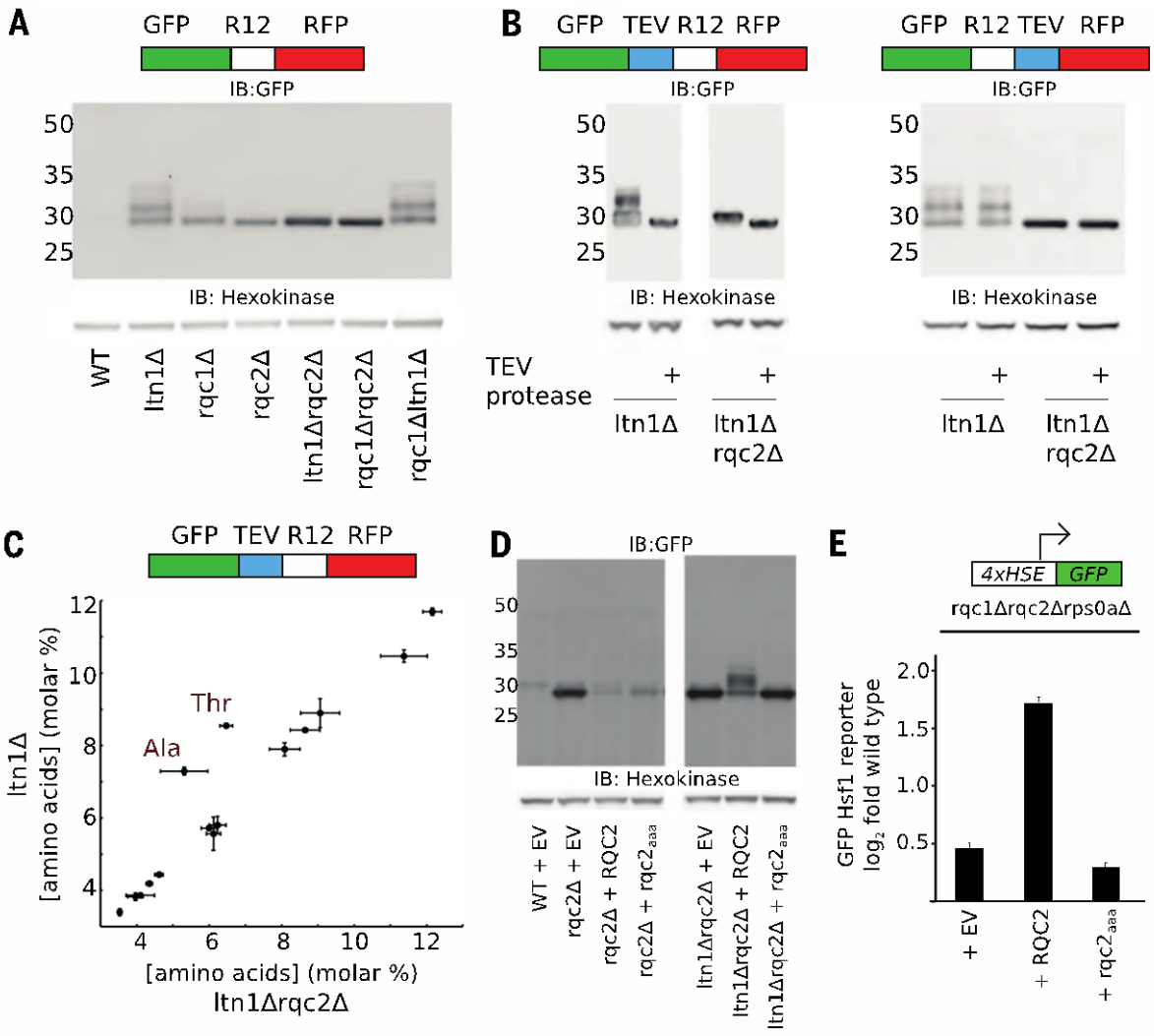

Fig. 4. Rqc2p-dependent formation of CAT tails. (A, B, and D) Immunoblots of stalling reporters in RQC deletion strains. (C) Total amino acid analysis of immunoprecipitated GFP expressed in ltn1D and ltn1Drqc2D strains, n = 3 independent immunoprecipitations. (E) Triplicate GFP levels measured with a flow cytometer and normalized to a wild-type control. EV, empty vector. All error bars are standard deviations.

Materials and Methods

S. cerevisiae strains

Strain	Background	Plasmid 1	Plasmid 2	Stalling sequence
yOBj065	BY4741	pTDH3-GFP_R12_RFP, URA3 marker		cgg cga cga cgg cga cgc cga cga cga cgg cgc cgc
yOBj067	BY4741 *ltn1::kan*	pTDH3-GFP_R12_RFP, URA3 marker		cgg cga cga cgg cga cgc cga cga cga cgg cgc cgc
yOBj068	BY4741 *rqc1::nat*	pTDH3-GFP_R12_RFP, URA3 marker		cgg cga cga cgg cga cgc cga cga cga cgg cgc cgc
yOBj069	BY4741 *rqc2::kan*	pTDH3-GFP_R12_RFP, URA3 marker		cgg cga cga cgg cga cgc cga cga cga cgg cgc cgc
yOBj070	BY4741 *ltn1::kan rqc2::nat*	pTDH3-GFP_R12_RFP, URA3 marker		cgg cga cga cgg cga cgc cga cga cga cgg cgc cgc
yOBj072	BY4741 *rqc1::nat rqc2::kan*	pTDH3-GFP_R12_RFP, URA3 marker		cgg cga cga cgg cga cgc cga cga cga cgg cgc cgc
yOBj071	BY4741 *rqc1::nat ltn1:kan*	pTDH3-GFP_R12_RFP, URA3 marker		cgg cga cga cgg cga cgc cga cga cga cgg cgc cgc
yOB520	BY4741 *ltn1::kan*	pTDH3-GFP_TEV_R12_RFP, URA3 marker		cgg cga cga cgg cga cgc cga cga cga cgg cgc cgc
yOBj020	BY4741 *ltn1::kan rqc2::nat*	pTDH3-GFP_TEV_R12_RFP, URA3 marker		cgg cga cga cgg cga cgc cga cga cga cgg cgc cgc
yOBj073	BY4741 *ltn1::kan*	pTDH3-GFP_R12_TEV_RFP, URA3 marker		cgg cga cga cgg cga cgc cga cga cga cgg cgc cgc
yOBj043	BY4741	pTDH3-GFP_TEV_R12_RFP, URA3 marker	pRS315 empty vector, LEU2 marker	cgg cga cga cgg cga cgc cga cga cga cgg cgc cgc
yOBj047	BY4741 *rqc2::kan*	pTDH3-GFP_TEV_R12_RFP, URA3 marker	pRS315 empty vector, LEU2 marker	cgg cga cga cgg cga cgc cga cga cga cgg cgc cgc
yOBj048	BY4741 *rqc2::kan*	pTDH3-GFP_TEV_R12_RFP, URA3 marker	pRQC2-RQC2_WT, LEU2 marker	cgg cga cga cgg cga cgc cga cga cga cgg cgc cgc
yOBj049	BY4741 *rqc2::kan*	pTDH3-GFP_TEV_R12_RFP, URA3 marker	pRQC2-RQC2_hpa (D9A, D98A, R99A), LEU2 marker	cgg cga cga cgg cga cgc cga cga cga cgg cgc cgc
yOBj051	BY4741 *ltn1::kan rqc2::nat*	pTDH3-GFP_TEV_R12_RFP, URA3 marker	pRS315 empty vector, LEU2 marker	cgg cga cga cgg cga cgc cga cga cga cgg cgc cgc
yOBj052	BY4741 *ltn1::kan rqc2::nat*	pTDH3-GFP_TEV_R12_RFP, URA3 marker	pRQC2-RQC2_WT, LEU2 marker	cgg cga cga cgg cga cgc cga cga cga cgg cgc cgc
yOBj053	BY4741 *ltn1::kan rqc2::nat*	pTDH3-GFP_TEV_R12_RFP, URA3 marker	pRQC2-RQC2_hpa (D9A, D98A, R99A), LEU2 marker	cgg cga cga cgg cga cgc cga cga cga cgg cgc cgc
yOB255	BY4741 *ura3::HSEEmGFP*			
yOBj059	BY4741 *ura3::HSEEmGFP rqc2::kan rqc1::nat rps0a::hyg*	pRS315 empty vector, LEU2 marker		

Strain	Background	Plasmid 1	Plasmid 2	Stalling sequence
yOBj060	BY4741 *ura3::HSEEmGFP rqc2::kan rqc1::nat rps0a::hyg*	pRQC2-RQC2_WT, LEU2 marker		
yOBj061	BY4741 *ura3::HSEEmGFP rqc2::kan rqc1::nat rps0a::hyg*	pRQC2-RQC2aaa (D9A, D98A, R99A), LEU2 marker		
yOB542	BY4741 *rqc1-3xFLAG::kan ltn1ΔRING::nat*			
yOB462	BY4741 *rqc1-3xFLAG::kan rqc2::nat*			
yPS1234	BY4741 *rqc1-3xFLAG::kan vms1::nat rqc2-PrA::his5*	pJR3462-VMS1-GFP, URA3 marker		
yPS1250	BY4741 *rqc1-3xFLAG::kan rqc2::nat*	pRS315 empty vector, LEU2 marker		
yPS1251	BY4741 *rqc1-3xFLAG::kan rqc2::nat*	pRQC2-RQC2_WT, LEU2 marker		
yPS1252	BY4741 *rqc1-3xFLAG::kan rqc2::nat*	pRQC2-RQC2_aaa (D9A, D98A, R99A), LEU2 marker		
yOBj142	BY4741	pTDH3-GFP_TEV_R4_RFP, URA3 marker		cga cga cga cga ata aat aaa ata gat aga
yOBj143	BY4741 *ltn1::kan*	pTDH3-GFP_TEV_R4_RFP, URA3 marker		cga cga cga cga ata aat aaa ata gat aga
yOBj144	BY4741 *rqc2::kan*	pTDH3-GFP_TEV_R4_RFP, URA3 marker		cga cga cga cga ata aat aaa ata gat aga
yOBj145	BY4741 *ltn1::kan rqc2::nat*	pTDH3-GFP_TEV_R4_RFP, URA3 marker		cga cga cga cga ata aat aaa ata gat aga
yOBj025	BY4741 *ltn1::kan*	pTDH3-GFP-Rz-His3		
yOBj028	BY4741 *ltn1::kan rqc2::nat*	pTDH3-GFP-Rz-His3		

Supplementary Figure 1

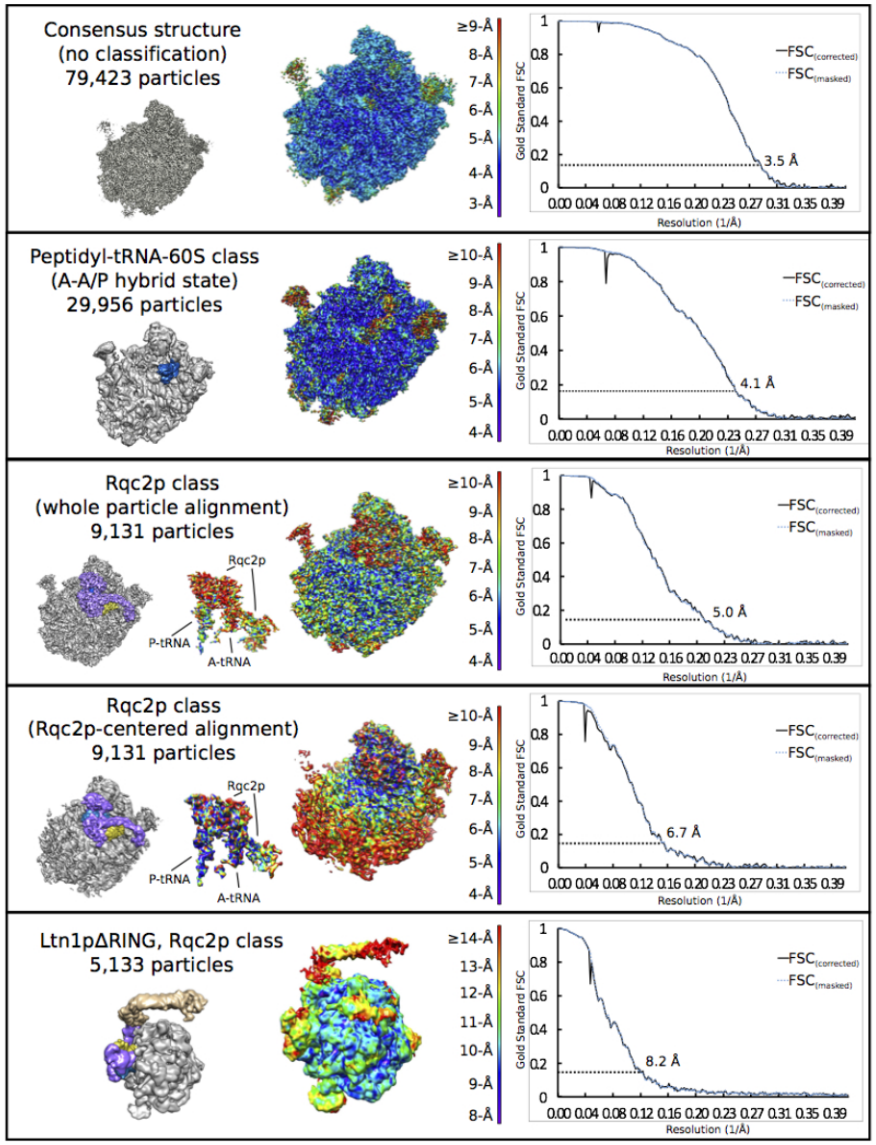

Fig S1. Reconstruction statistics of RQC-related structures. Number of particles, surface views, local resolution heat maps, and FSC plots shown. 'Gold standard' FSC cutoffs at 0.143 indicated by dashed lines. Extra-ribosomal densities colored as in Figure 1.

Supplementary Figure 2

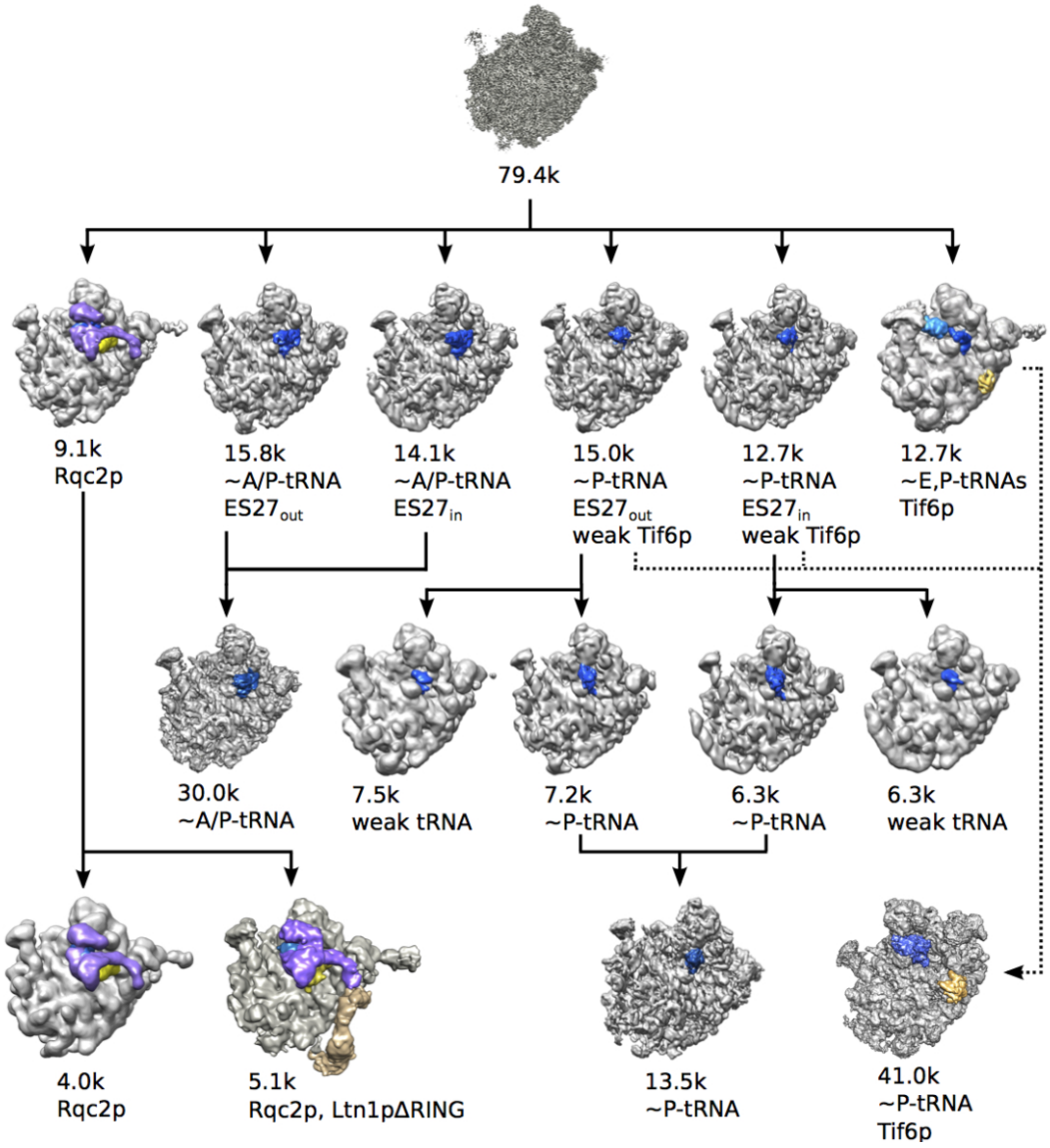

Fig S2. 3D classification scheme. Flow chart depicting 3D classification from an initial consensus structure, revealing distinct classes containing tRNA(s), Tif6p, Rqc2p, and Ltn1pΔRING.

Supplementary Figure 3

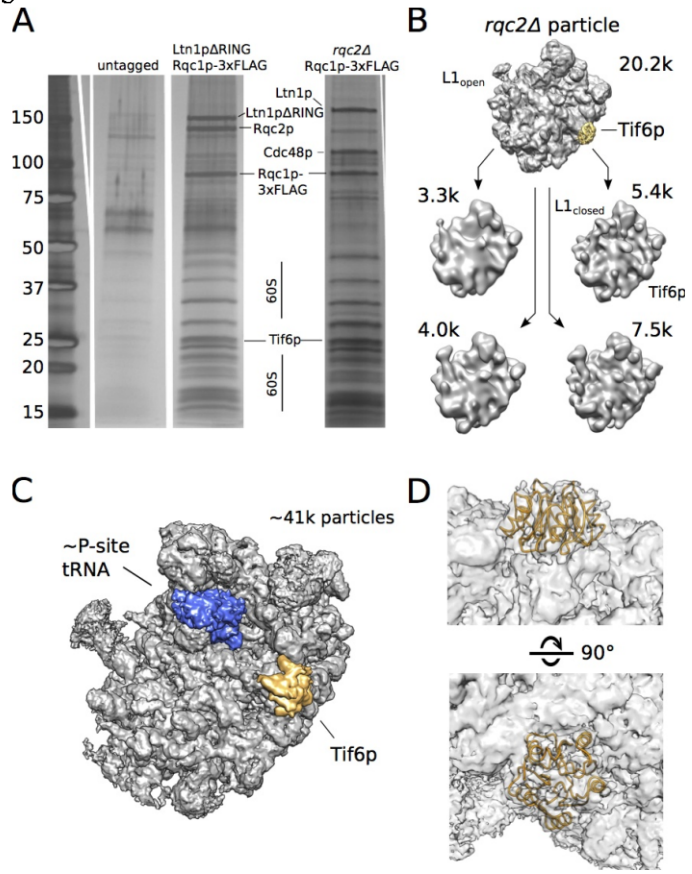

Fig S3. Co-immunoprecipitation and structures of *rqc2Δ* or Tif6p-containing particles.

(A) Silver stained Ltn1ΔRING and *rqc2Δ* samples following αFLAG co-immunoprecipitation. Pertinent protein bands labeled; co-IP of untagged yeast shown to indicate background contaminant bands. **(B)** Cryo-EM reconstruction of the *rqc2Δ* RQC particle with the anti-association factor Tif6p density indicated. **(C)** Refined 'crown view' structure of the 3D class containing Tif6p bound to peptidyl-tRNA-60S (from the Rqc1-FLAG, Ltn1ΔRING strain; see bottom right of Fig. S2). **(D)** Tif6p crystal structure (orange ribbon, PDB entry 4A18 (*40*)) fit within the cryoEM density.

Supplementary Figure 4

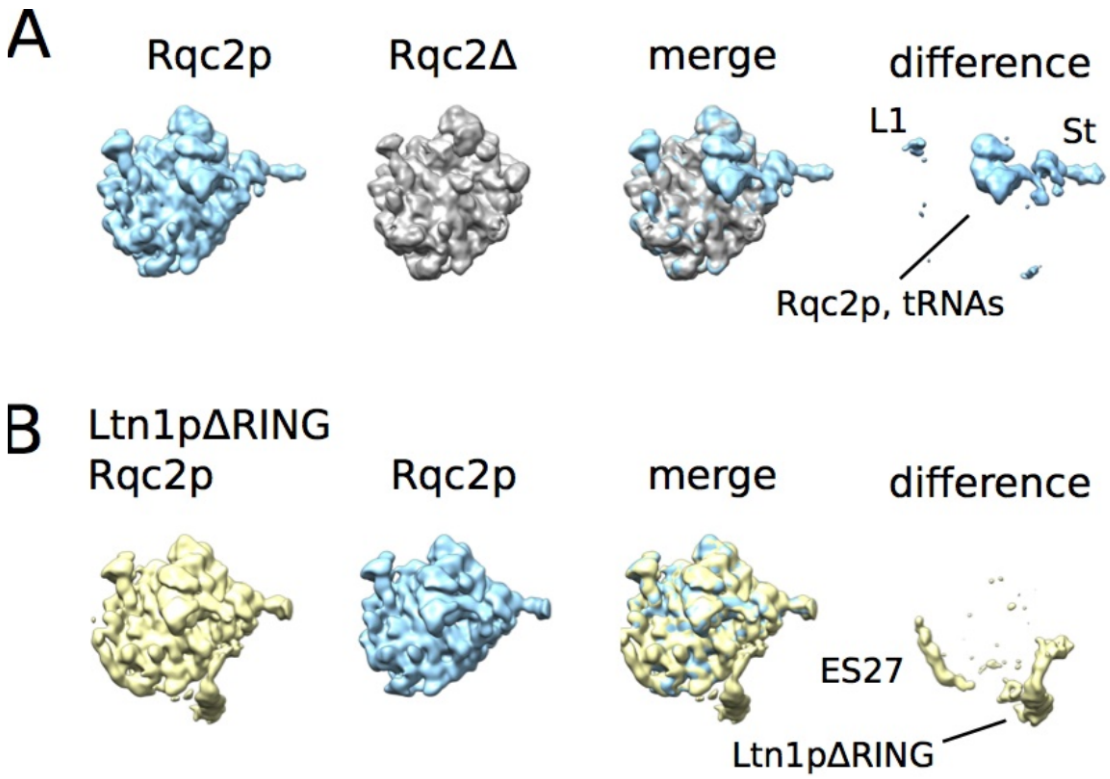

Fig S4. Identification of RQC factors by difference mapping. (A) Rqc2p density isolated by computing the difference between Rqc2p and Rqc2Δ structures. (B) Ltn1pΔRING density isolated by computing the difference between Rqc2p-classified structures (see bottom left of Fig. S2).

Supplementary Figure 5

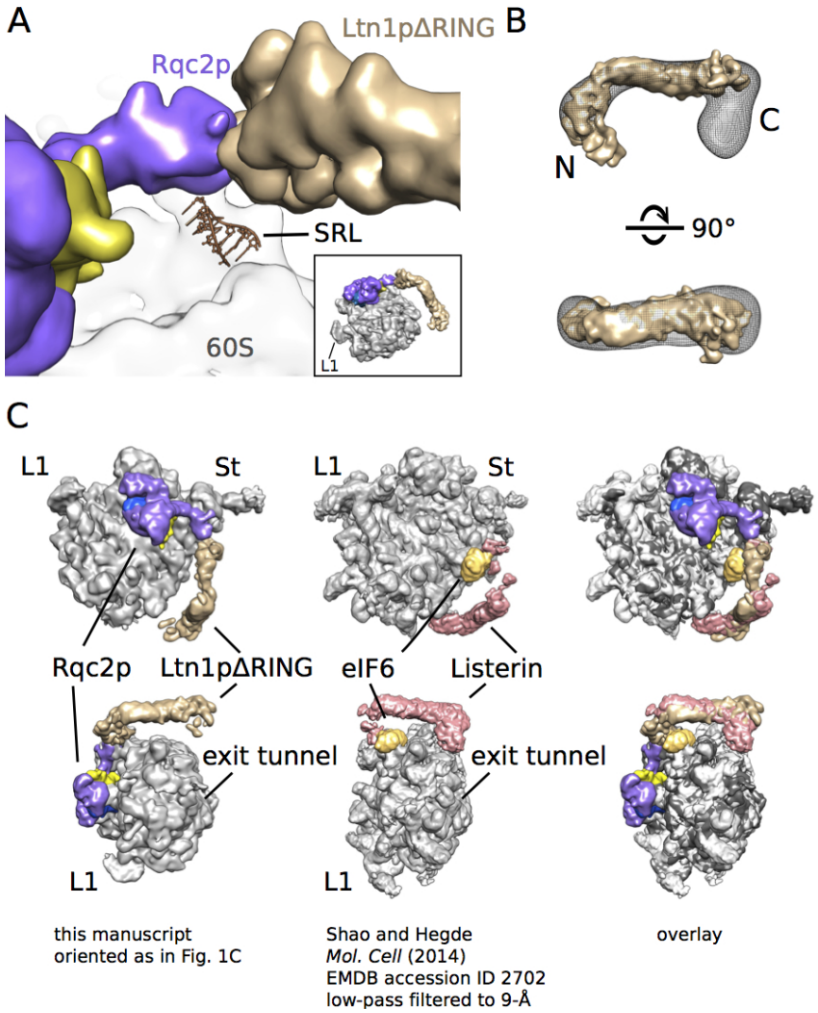

Fig. S5. Ltn1pΔRING structure analysis. (A) Ltn1pΔRING connects with Rqc2p and the 60S subunit at the sarcin-ricin loop (SRL). Inset specifies view. **(B)** Structural comparison between the 60S-bound Ltn1pΔRING and solution structure of Ltn1p (EMD-2252, (*6*)). Amino-(N) and carboxy-(C) termini indicated. **(C)** Structural comparison between the yeast 60S-bound Ltn1pΔRING and mammalian 60S-bound Listerin (*7*). L1 = L1 stalk; St = P-stalk

Supplementary Figure 6

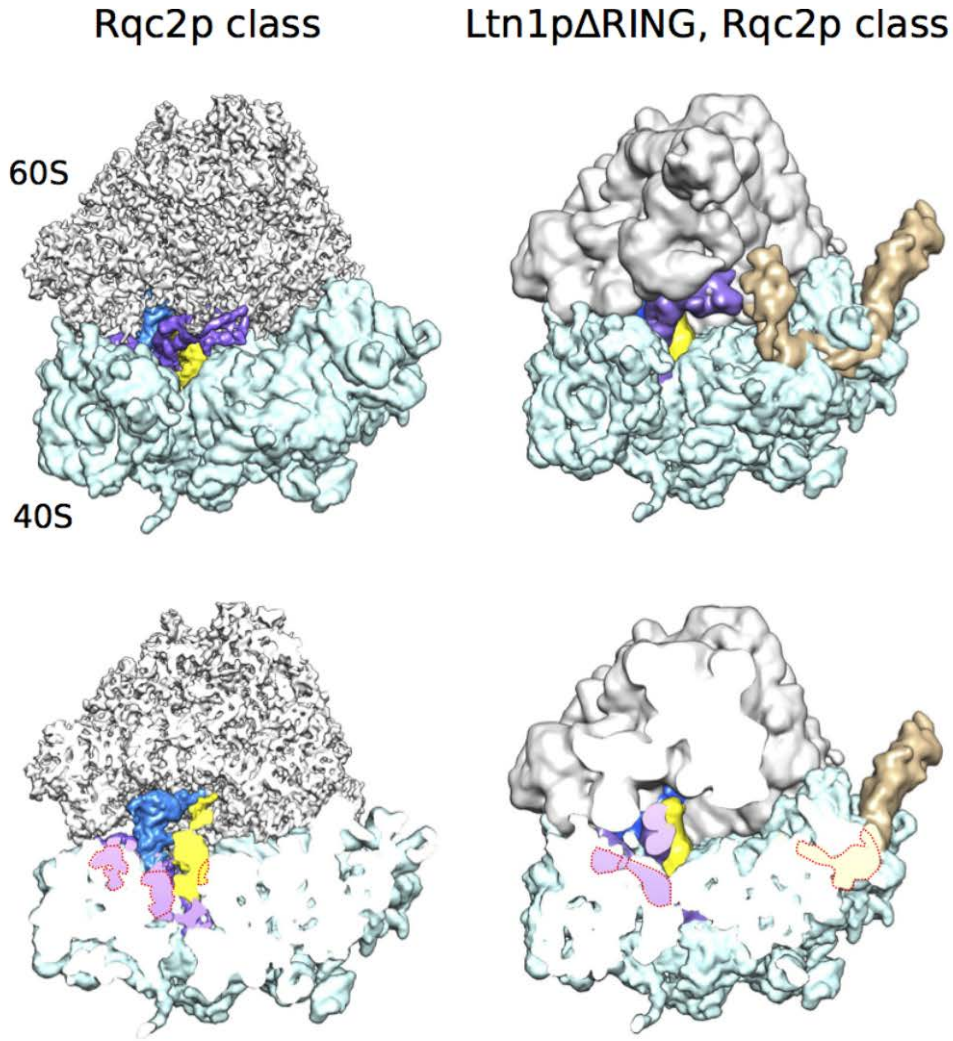

Figure S6. RQC binding is incompatible with 80S ribosomes. 40S (light blue) docked over 60S-Rqc2p and 60S-Rqc2p-Ltn1pΔRING structures. Top, surface views. Bottom, cut-away views. Representative clashes indicated by dotted red line.

Supplementary Figure 7

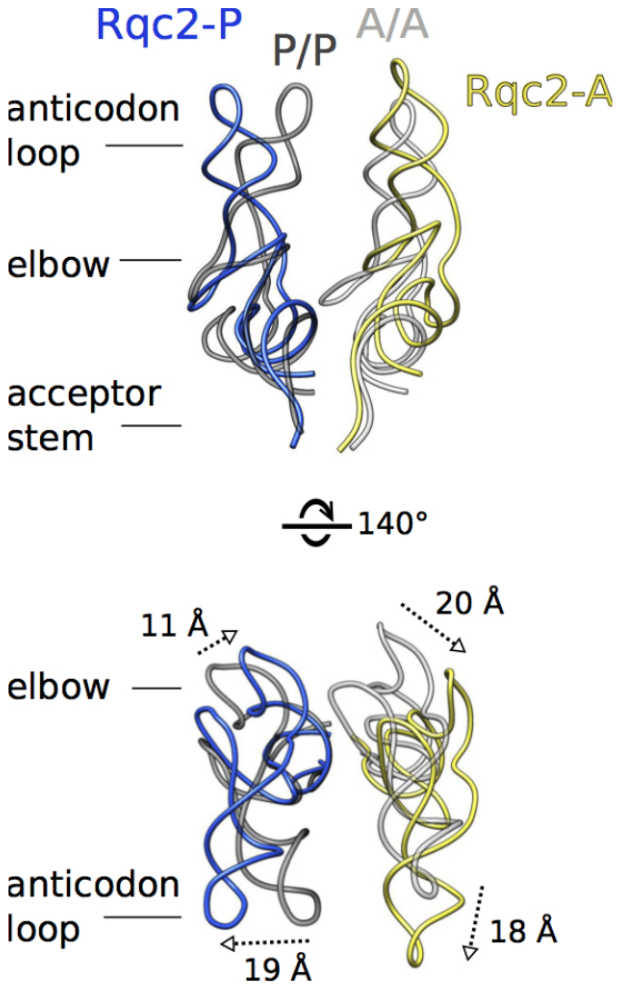

Fig S7. Comparison of Rqc2p-bound tRNAs with canonical A/A, P/P tRNA states. Top, Rqc2p-bound tRNAs colored and viewed as in Fig. 2B. Classical A/A (light grey) and P/P (dark grey) tRNAs superimposed. Bottom, rotated view indicates displacement of elbows and anticodon loops between classical and Rqc2p-bound tRNAs.

Supplementary Figure 8

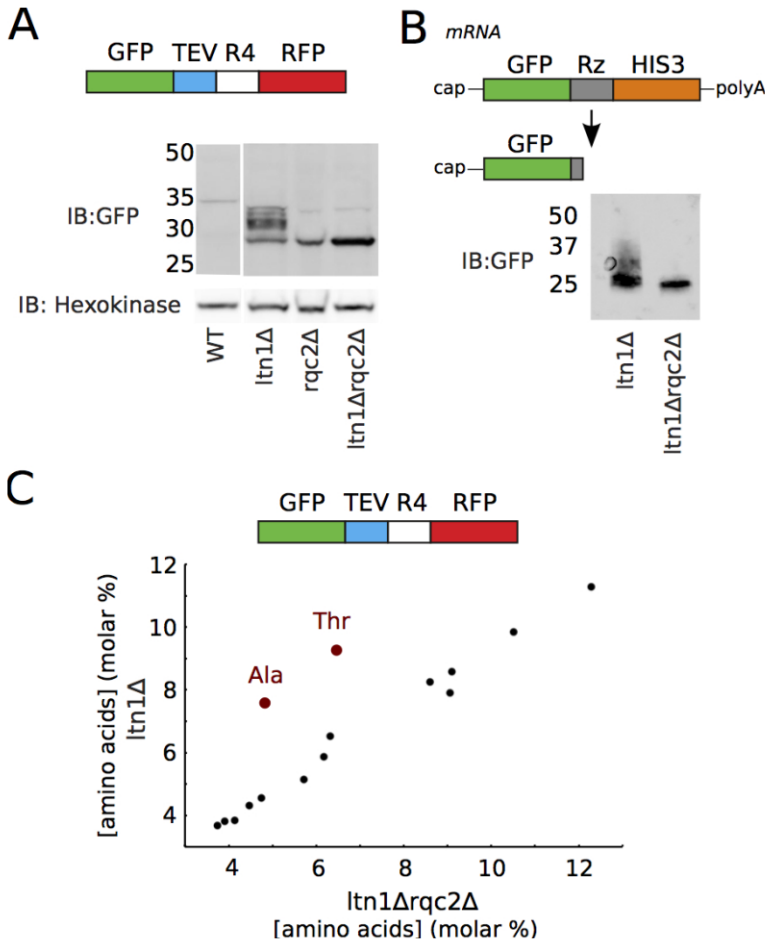

Fig S8. Rqc2p-mediated extensions persist in reporters containing CGA repeats or lacking a stop codon. (A) Immunoblot analysis of a stalling reporter encoding four consecutive CGA codons. This reporter was also designed to encode STOP codons upon +1 or +2 frame shifting. (B) Immunoblot analysis of the nonstop GFP-Rz reporter derived from the hammerhead ribozyme sequence (*19*). (C) Total amino acid analysis of the R4 stalling reporter, shown in (A). Also note that frame shifting of this mRNA could not lead to translation of alanine codons.

Cell lysis

Cells were grown in either rich media or synthetic dropout media and harvested at OD_{600} of ~1.5. The cells were pelleted at 4,500 x g for 6 minutes, washed in ice cold water, pelleted again at 4,000 x g for 6 minutes, then resuspended in lysis buffer (50mM HEPES-KOH pH 6.8, 150mM KOAc, 2mM $Mg(OAc)_2$, 1mM $CaCl_2$, 0.2M sorbitol, supplemented with cOmplete protease inhibitor cocktail (Roche). Cell droplets were frozen in liquid nitrogen, lysed into powder using a Freezer/Mill® (SPEX SamplePrep), and stored at -80°C until use.

Supplementary Figure 9

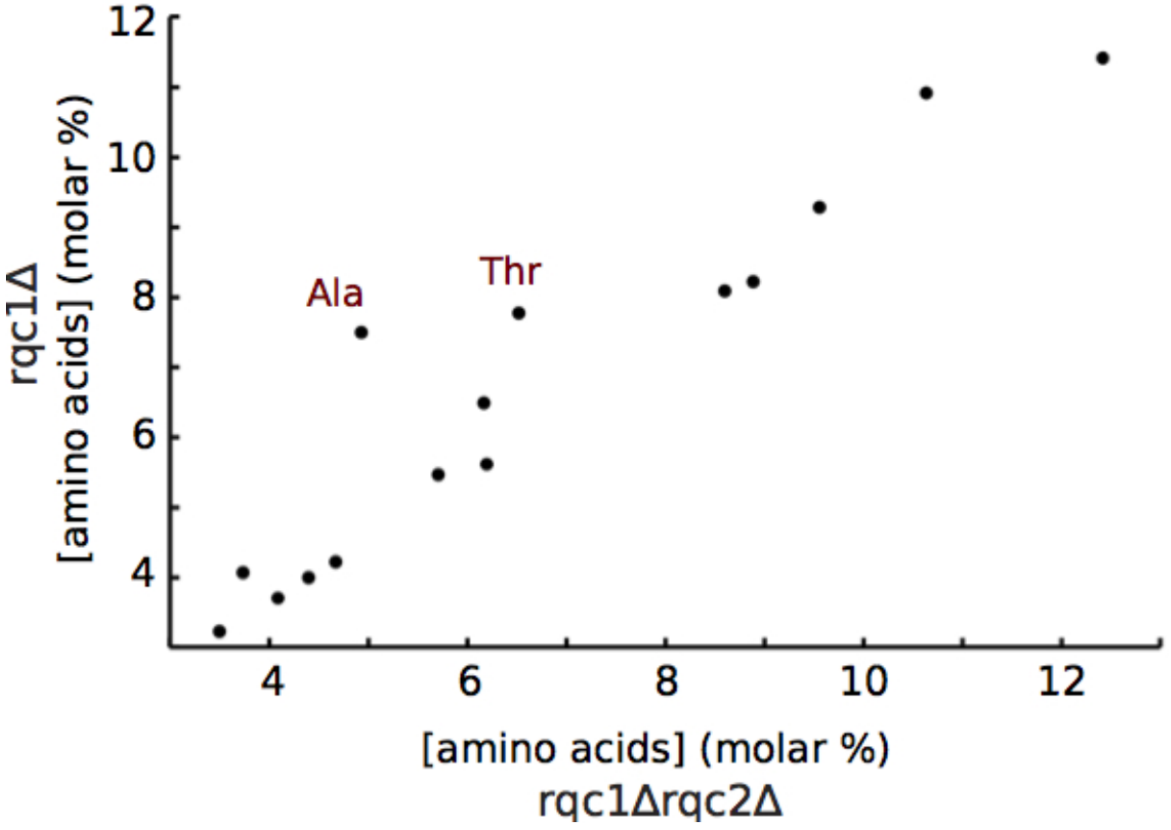

Fig S9. CAT tail formation in rqc1Δ cells. Amino acid analysis of GFP-TEV-R12-RFP in rqc1Δ and rqc1Δrqc2Δ backgrounds. Ala and Thr residues indicated.

Supplementary Figure 10

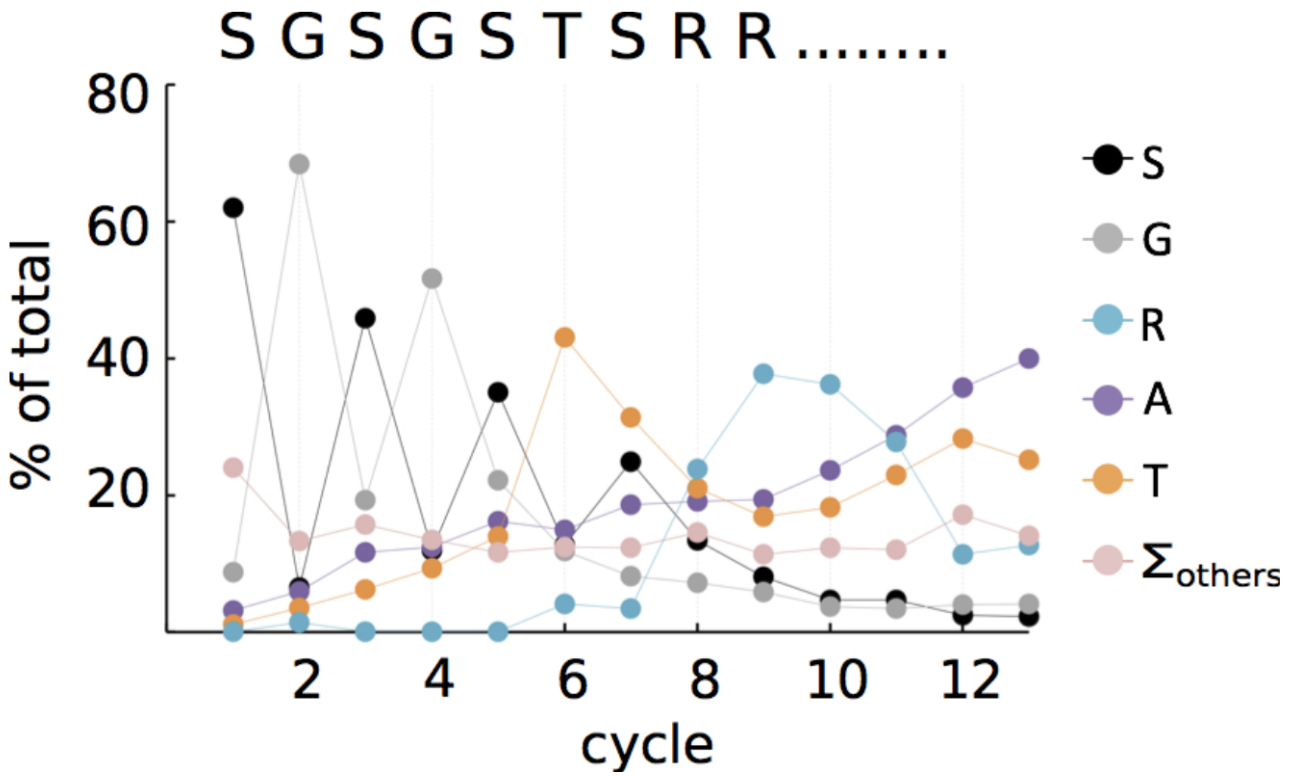

Fig S10. Edman degradation sequencing of TEV-released CAT tails. Each cycle represents an average of two replicates and shows the proportion of residues versus the sum of all amino acids. Note that SGSGSTS is the plasmid-encoded TEV linker upstream of the R12 stall.

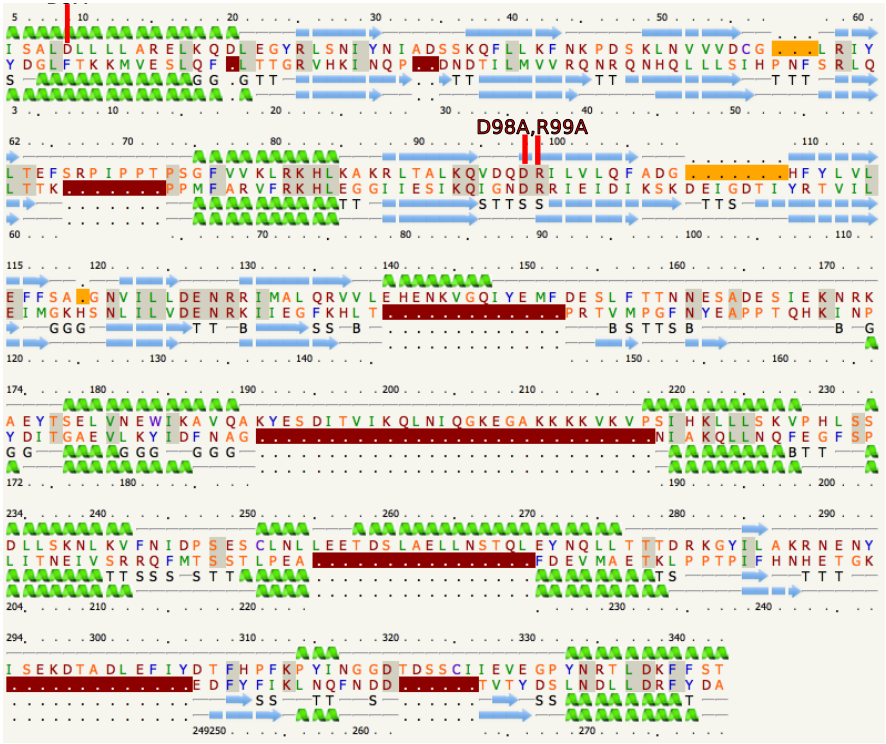

ence-to-structure alignment was generated with Phyre2 (*41*).

Supplementary Figure 12

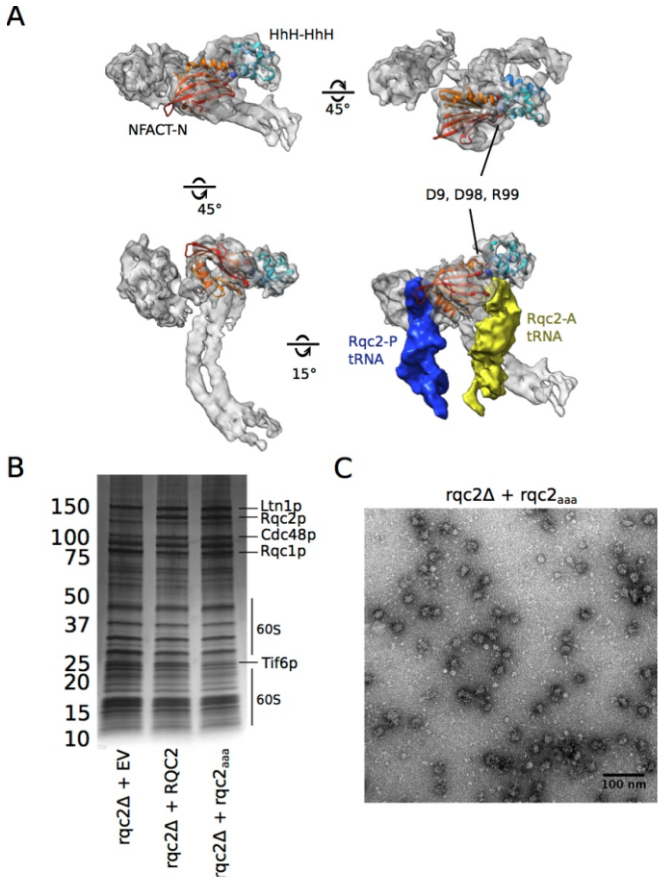

Fig S12. Rqc2p NFACT-N modeling and RQC IP of *rqc2*$_{aaa}$. (A) Rigid-body fits of the NFACT-N and tandem HhH lobes of the Fbp structure (PDB entry 3DOA, ribbon representation) docked within the Rqc2p cryoEM density. Rqc2p and the tRNA densities were segmented automatically with the Segger algorithm as implemented within UCSF Chimera (*33*, *35*). D9, D98, R99 are shown as space filling models. (B) Silver stained SDS-PAGE of Rqc1p-FLAG IPs from *rqc2Δ* backgrounds re-expressed with empty vector (EV), WT RQC2, and *rqc2*$_{aaa}$. (C) Negative stain electron microscopy field of RQC particles purified from *rqc2Δ* strains harboring the *rqc2*$_{aaa}$ plasmid.

Supplementary Figure 13

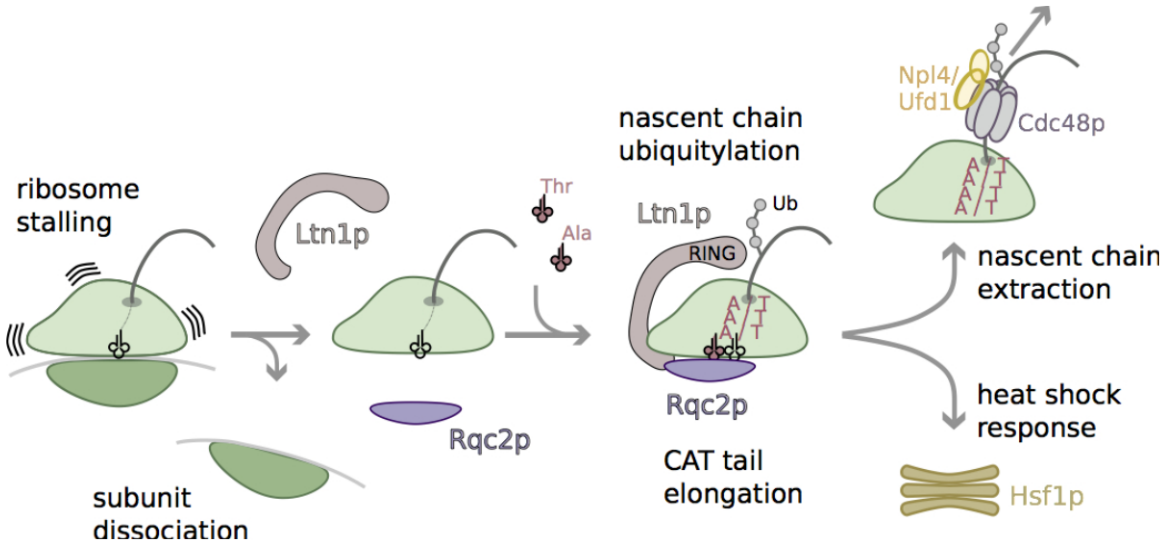

Fig S13. Schematic model for RQC-mediated recognition and rescue of stalled ribosomes. The 80S ribosome stalls during translation and the 40S dissociates. Ltn1p and Rqc2p recognize unique features of the resulting peptidyl-tRNA-60S complex. Ltn1p binds Rqc2p and the 60S at the SRL and reaches around the 60S towards the exit tunnel to ubiquitylate emerging nascent chains. Cdc48p and its co-adaptors target the ubiquitylated peptide to the proteasome for degradation. Rqc2p binds the exposed ~P-site tRNA, and directs elongation of the stalled nascent chain with CAT tails by recruiting $tRNA^{Ala(IGC)}$ and $tRNA^{Thr(IGU)}$ to the A-site. Rqc2p directed translation elongation is mRNA template-free and 40S-free. The resulting CAT tail is involved in signaling to Heat Shock Factor 1, Hsf1p.

Table S1

Nano-ESI-FT-ICR data of trypsin-released CAT tails

CAT tail peptide length	amino acid composition	theoretical mass (Da)	observed mass (Da)	ppm difference (observed vs theoretical)
5	4A, 1T	403.2067	403.2071	1.0
6	3A, 3T	534.2649	534.2656	1.3
6	4A, 2T	504.2544	504.2554	2.0
6	5A, 1T	474.2438	474.2445	1.5
7	5A, 2T	575.2915	575.2925	1.7
7	6A, 1T	545.2809	545.2816	1.3
8	6A, 2T	646.3286	646.3294	0.8
9	7A, 2T	717.3657	717.3666	1.3
12	5A, 7T	1080.5299	1080.5310	1.0
12	6A, 6T	1050.5193	1050.5214	2.0
12	7A, 5T	1020.5087	1020.5096	0.9
13	6A, 7T	1151.5670	1151.5696	2.3
13	7A, 6T	1121.5564	1121.5584	1.8
14	8A, 6T	1192.5935	1192.5962	2.3
19	11A, 8T	1607.8002	1607.8036	2.1

RQC immunoprecipitation

RQC particles were purified as described (*1*). Yeast powder was thawed on ice and resuspended in immunoprecipitation buffer: 100mM KOAc, 10mM $MgCl_2$, 25mM HEPES-KOH pH 7.4, 0.5mM DTT, supplemented with cOmplete protease inhibitors (Roche). Supernatant was clarified by centrifugation and incubated with anti-FLAG M2 agarose resin (Sigma) or IgG-coated magnetic Dynabeads (Life Technologies) for 1 hour at 4°C. Resins were washed thoroughly and the RQC particles were eluted with excess 3xFLAG peptide (Rqc1p-3XFLAG) or by incubation with HRV 3C protease (Rqc2p-ProteinA) for 1 hour at 4°C. Purified samples were verified by silver stain SDS-PAGE and negative stain electron microscopy and used immediately for cryo-EM experiments.

Electron microscopy

RQC particles suffered from different orientation biases on ultrathin carbon-coated lacey grids versus when suspended in the holes of Quantifoil holey carbon grids. Thus, we used both types of grids to obtain a wider distribution of particle views. In brief, 4.5µl of purified RQC were applied to either glow-discharged lacey carbon grids with an ultrathin layer of carbon deposited on top (Ted Pella) or to chloroform-washed, non-glow-discharged Quantifoil R2/2 grids (SPI Supplies). RQC particles only entered the holes of hydrophobic grids washed with chloroform. Uniformly thin ice was achieved by manually spreading the sample droplet across the grid surface using a pipette tip and by applying the sample to both sides of the grid. Grids of both types were plunge frozen in liquid ethane using a Vitrobot III system (FEI) (40s wait time, 3.0s blot time, operating at 4°C and 75% relative humidity) and stored in liquid nitrogen.

The *rqc2Δ* dataset was collected on an FEI Titan Krios operating at 300kV equipped with a Falcon I direct electron detector. Images were recorded automatically using EPU (FEI) at a nominal magnification of 47,000×, which corresponds to a pixel size of 1.37 Å. The dataset ranged between 0.8 to 2.5µm under focus and each micrograph had a total dose of ~25 electrons per $Å^2$.

The Rqc1p-3XFLAG and Rqc2p-ProteinA datasets were collected on a Tecnai Polara (FEI) operating at 300kV, equipped with the K2 Summit direct electron detector (Gatan), as described (*27*). Images were recorded using the acquisition program UCSFImage4 (written by X. Li (*27*)), with a defocus range from 0.8 to 2.0µm. We recorded movies in super-resolution counting mode at a magnification of 31,000×, which corresponds to a physical pixel size of 1.22 Å. The beam intensity was set to ~8 counts per physical pixel per second, corresponding to a dose rate of ~10 electrons per physical pixel per second. Movies were recorded as a stack of 24 subframes, each of which was accumulated for 0.2 s, resulting in an average of ~1.7 counts per physical pixel in each subframe and a total specimen dose of ~35 electrons per $Å^2$. All subframes per movie were motion corrected as implemented within UCSFImage4.

Image processing and 3D reconstruction

CTF parameters for micrographs were determined using the program CTFFIND (*28*). The power spectrum for each micrograph was visually inspected and those with poor Thon rings were rejected from downstream analysis. Particle images were extracted from micrographs in a semi-automated manner using the *swarm* tool in *e2boxer.py* as part of the EMAN2 package (*29*).

All 2D and 3D classifications and refinements were performed using the RELION package (*30*). Particles were sorted into 2D classes, followed by rejecting non-60S particles (i.e., incoherent particles and contaminant 80S particles) from downstream analysis. The remaining particles were then used to compute a consensus 3D reconstruction, after which the aligned particles were 3D classified in an unsupervised manner. Individual classes were then further refined until convergence using the auto-refine procedure in RELION. Because particle alignment is dominated by the larger 60S structure, we further applied a soft spherical mask around the Rqc2p density in order to improve the quality of the extra-ribosomal features (at the expense of a lower resolution ribosome). Local resolution of each map was computed using ResMap (*31*), using unfiltered map halves as outputted by RELION. Difference maps were calculated using Bsoft (*bop* program (*32*)).

Structure visualization and modeling

Rigid body fittings were done in UCSF Chimera (*33*). Extra-ribosomal densities were distinguished by computing difference maps between cryoEM reconstructions and reference yeast 60S maps from crystal structure coordinates (PDB entries 3U5D & 3U5E (*34*)). Individual components (i.e., Rqc2p, Ltn1p, tRNAs, nascent chains) were isolated using the Segger tools as implemented within UCSF Chimera (*33*, *35*).

Based on predicted structural conservation between the N-terminal domain of Rqc2p and other members of the NFACT family of proteins, we first manually guided the fitting of the NFACT-N domain of the Fbp crystal structure (PDB entry 3DOA, residues 1-140) into the Rqc2p density, and then used UCSF Chimera to refine the rigid-body fitting. tRNA structures were obtained from PDB entry 2J00 (*36*) and fitted as rigid bodies into reconstructions using UCSF Chimera (*33*).

TGIRT-seq of RQC-associated RNAs

Total RNA isolated from RQC particles that had been purified from RQC2 and *rqc2Δ* strains was analyzed by deep sequencing using a thermostable group II intron reverse transcriptase (TGIRT) for RNA-seq library construction (*9*, *37*). The TGIRT enhances read through of modified or edited tRNA bases, facilitating generation of full-length cDNA copies of tRNAs, and it initiates reverse transcription by a template-switching mechanism that is sensitive to whether or not the 3' end of the tRNA is aminoacylated. Total RNAs were extracted from the purified RQC by using Trizol. Purified RNAs were precipitated with isopropanol, washed in 75% ethanol, and dissolved in water. Half of the sample was deacylated by incubation in 0.1 M Tris-HCl (pH 9.0) for 45 min at 37°C, as described (*38*). Portions of the purified RNA samples before and after deacylation were analyzed with the Small RNA Analysis Kits on a 2100 Bioanalyzer (Agilent Technologies) to assess the relative abundance of tRNAs to 5S rRNA and 5.8S rRNA.

The construction of RNA-seq libraries via TGIRT template switching was done essentially as described (*9*, *37*). The initial template-primer substrate for template-switching reactions consists of a 41-nt RNA oligonucleotide (5'-AGA UCG GAA GAG CAC ACG UCU AGU UCU ACA GUC CGA CGA UC/3SpC3/-3') with Illumina Read1 and Read2 primer binding sites and a 3' blocking group (three carbon spacer; IDT) annealed to a complementary 42-nt ^{32}P-labeled DNA primer, which leaves an equimolar mixture of A, C, G, or T single-nucleotide 3' overhangs. Reactions were done with RQC RNA (~100-200 ng), initial template-primer substrate (100 nM), TGIRT (TeI4c-MRF RT with a C-terminal truncation of the DNA endonuclease domain; 1 µM, 5 units/µl) and 1 mM dNTPs (an equimolar mix of dATP, dCTP, dGTP, and dTTP) in 20 µl of reaction medium containing 450 mM NaCl, 5 mM $MgCl_2$, 20 mM Tris-HCl, pH 7.5, 1 mM DTT. After pre-incubating a mixture of all components except dNTPs at room temperature for 30 min, reactions were initiated by adding dNTPs, incubated at 60°C for 30 min, and terminated by adding 5 M NaOH to a final concentration of 0.25 M, incubating at 95°C for 3 min, and then

neutralizing with 5 M HCl. The labeled cDNAs were analyzed by electrophoresis in a denaturing 6% polyacrylamide gel, which was scanned with a Typhoon FLA9500 phosphorImager (GE Healthcare). Gel regions containing cDNAs with sizes of ~60-nt and ~61-190-nt, including the 42-nt primer added by template-switching, were electroeluted using a D-tube Dialyzer Maxi with MWCO of 6-8 kDa (EMD Millipore) and ethanol precipitated in the presence of 0.3 M sodium acetate and linear acrylamide carrier (25 µg; Thermo Scientific). The purified cDNAs were then circularized with CircLigase II (Epicentre; manufacturer's protocol with an extended incubation time of 5 h at 60°C), extracted with phenol-chloroform-isoamyl alcohol (25:24:1) and ethanol precipitated. The circularized cDNA products were amplified by PCR with Phusion-HF (Thermo Scientific) using Illumina multiplex (5'- AAT GAT ACG GCG ACC ACC GAG ATC TAC ACG TTC AGA GTT CTA CAG TCC GAC GAT C -3') and barcode (5'- CAA GCA GAA GAC GGC ATA CGA GAT BARCODE GTG ACT GGA GTT CAG ACG TGT GCT CTT CCG ATC T -3') primers under conditions of initial denaturation at 98°C for 5 s, followed by 12 cycles of 98°C for 5 s, 60°C for 10 s and 72°C for 10 s.

Samples were sequenced on an Illumina MiSeq or HiSeq (100-nt single end reads). Read quality was assessed using FastQC (see http://www.bioinformatics.babraham.ac.uk/projects/fastqc). Reads were trimmed and filtered to remove contaminant primer sequences and substandard base calls from the 3' ends using Fastx-Toolkit (see http://hannonlab.cshl.edu/fastx_toolkit) and Ea-utils (http://code.google.com/p/ea-utils), respectively. Trimmed and filtered reads were aligned to the yeast genome reference sequence (Ensembl EF4) with Bowtie 2 using end-to-end alignment, yielding 0.5-2 million (MiSeq) or 2-4 million (HiSeq) mapped reads.

Western Blots

Yeast were grown to saturation overnight in SD-URA media, diluted to OD_{600} 0.1 in the morning, and grown for 3-5 hours to OD_{600} 0.5. The cultures were then normalized to 5ml of OD_{600} 0.2, pelleted by centrifugation, resuspended in 20µl NuPAGE® LDS Sample Buffer (Life Technologies), and lysed by boiling for 5 minutes. The samples were centrifuged and 5ul of supernatant was loaded into NuPAGE® Novex® 4-12% Bis-Tris Precast protein gels (Life Technologies).

The proteins were transferred onto Novex® nitrocellulose membranes (Life Technologies) using the Trans-Blot® Turbo™ Transfer System (Bio-Rad). The membranes were blocked in 5% nonfat milk in TBST for 1 hour, incubated overnight in primary antibodies (αGFP, MA5-15256, Pierce and α-Hexokinase, H2035-01, US Biological), washed in TBST for 10 minutes, incubated in DyLight secondary antibodies (Pierce) for 1 hour, and washed 3 times in TBST for 5 minutes each. The membranes were visualized using the VersaDoc™ system (Bio-Rad).

TEV protease digestion

For the TEV reaction, 4µl of clarified lysate from frozen yeast powder was incubated with 2ul of ProTEV Plus (Promega) with 1mM DTT at room temperature for 2 hours. 6.6µl of NuPAGE® LDS Sample Buffer (Life Technologies) was added, and the samples were boiled for 5 minutes. The samples were centrifuged and 5µl of supernatant was loaded into NuPAGE® Novex® 4-12% Bis-Tris Precast protein gels (Life Technologies).

Amino Acid Analysis

Frozen yeast lysate powder was prepared, resuspended, and clarified as described above. 2ml of clarified lysate was incubated with 50µl of GFP-Trap® (Chromotek) for 1 hour at 4°C, and washed 3 times in IP buffer for 5 minutes each. The washed GFP-Trap® (Chromotek) resin was incubated for 2 minutes in IP buffer adjusted to pH 2.0 in order to acid-elute the samples.

Amino acid analysis was performed by UC Davis Genome Center using the following protocol, adapted from (*39*): samples were dried in a glass hydrolysis tube. The samples were then hydrolyzed in 6N HCl, 1% phenol at 110°C for 24hrs under vacuum. After hydrolysis, the samples were cooled, unsealed, and dried again. The dried samples were dissolved in 1mL sodium diluent (Pickering) with 40nmol/mL NorLeucine added as an internal standard. For each run, 50µl of sample was injected onto the ion-exchange column.

An amino acid standards solution for protein hydrolysate on the Na-based Hitachi 8800 (Sigma, A-9906) is used to determine response factors, and thus calibrate the Hitachi 8800 analyzer for all of the amino acids. In addition this standard has been verified against the National Institute of Standards and Technology (NIST) standard reference material 2389a.

Edman degradation sequencing

GFP IP was performed as described above. Washed GFP-Trap® (Chromotek) resin was incubated with ProTEV Plus (Promega) with 1mM DTT overnight at 4°C. The supernatant was collected and added to NuPAGE® LDS Sample Buffer (Life Technologies). Samples were boiled for 5 minutes, run on a NuPAGE® Novex® 12% Bis-Tris Precast gel (Life Technologies), and transferred to a PVDF membrane (Bio-Rad). The membrane was visualized with Coomassie blue staining. The low molecular weight band that ran at the gel front was excised and subject to Edman sequencing at Stanford University's Protein and Nucleic Acid Facility.

N-terminal sequence analysis is determined using Edman chemistry on an Applied Biosystems (AB) Procise liquid-pulse protein sequenator. PTH-Amino Acids are separated on a Brownlee C-18 reverse phase column (2.1 mm x 22 cm) at 55 C using a linear gradient of 14 to 44% buffer B over 17.6 min. Buffer A is 3.5% tetrahydrofuran and 2% AB premix buffer concentrate. (The recipe for the concentrate is proprietary to AB, but they have published the approximate composition as follows: 10-20% Acetic Acid, < 10% Sodium Acetate, < 10% Sodium Hexanesulfonate, 65-75% Water.) Buffer B is 12% Isopropanol in Acetonitrile. PTH-amino acid analysis is performed by Model 610A software, version 2.1.

GFP Fluorescence Measurements

Fluorescence was measured using a LSRII flow cytometer (BD). All fluorescent measurements were performed at 25°C at log phase in synthetic complete media (SC). Matlab 7.8.0 (Mathworks) was then used to compute the median internally-normalized values (GFP/sidescatter for the HSF reporter). Values were then normalized to WT and $\log_2$ scores computed, so that the wild-type strain had value 0. Error bars are standard deviations between technical replicates.

Trypsin Digestion

TEV-released CAT tails in solution were digested with TPCK-modified trypsin. Trypsin (in 50 mM NH_4HCO_3) was added to the solution, adjusted to pH 7.9 with dilute NH_4OH to obtain a ratio of approximately 1 to 25 (enzyme to protein). Digest reactions were allowed to continue over night at 37°C. Alternatively, gel bands of interest were excised, de-stained twice in 1 ml volumes of 50 mM NH_4HCO_3 in 50% methanol for 1 hour with gently mixing. Gel bands were then rehydrated in 1 ml of 50 mM NH_4HCO_3 for 30 min, cut into several pieces then dehydrated in 1 ml of 100% acetonitrile for 30 min at room temperature with gentle shaking. Acetonitrile was removed followed by the addition of 10 to 20 µl of sequence-grade modified trypsin (Promega) (20 ng/µL) in 50 mM NH_4HCO_3 and the gel pieces were allowed to swell for 15 minutes on ice. The excess trypsin solution was removed and the same 20 µl buffer (minus trypsin) was added to just cover the gel pieces, then incubated overnight at 37°C. The digestion was quenched by 20 µL of 1% formic acid, allowed to stand, and the supernatant collected. Further peptide extraction from the gel material was performed twice by the addition of 50% acetonitrile with 1% formic acid followed by sonication at 37°C for 20 minutes. A final complete dehydration of the gel pieces was accomplished by addition of 20 µL of 100% acetonitrile and incubation at 37°C for 20 minutes. All the extracts were pooled, dried and reconstituted in 100 µL of 5% acetonitrile with 0.1% formic acid for LC/MS/MS analysis.

Mass Spectrometry

Trypsin-digested peptides were analyzed using a nano-LC/MS/MS system comprised of a nano-LC pump (2D-ultra, Eksigent) and a LTQ-FT-ICR mass spectrometer (ThermoElectron Corporation, San Jose, CA). The LTQ-FT-ICR was equipped with a nanospray ion source (ThermoElectron Corp.).

Approximately 5 µL of tryptic digest samples were injected onto a dC18 nanobore LC column. The nanobore column was made in house using dC18 (Atlantis, Waters Corp); 3 µm particle; column: 75 µm ID x 100 mm length. A linear gradient LC profile was used to separate and elute peptides with a constant total flow rate of 350 nL/minute. The gradient consisted of 5 to 96% solvent B in 78 minutes (solvent B: 100% acetonitrile with 0.1% formic acid; solvent A: 100% water with 0.1% formic acid) was used for the analyses.

The LTQ-FT-ICR mass spectrometer was operated in the data-dependent acquisition mode with the "top 10" most intense peaks observed in an FT primary scan selected for on-the-fly MS/MS. Each peak is subsequently trapped for MS/MS analysis and peptide fragmentation in the LTQ linear ion trap portion of the instrument. Spectra in the FT-ICR were acquired from m/z

350 to 1400 Da at 50,000 resolving power. Mass accuracies are typically within about 3 ppm. The LTQ linear ion trap was operated with the following parameters: precursor activation time 30 ms and activation Q at 0.25; collision energy was set at 35%; dynamic exclusion width was set at low mass of 0.1 Da and high mass at 2.1 Da with one repeat count and duration of 10 s.

Mascot Database Searches

LTQ-FT/LC/MS/MS raw data files were processed with proteome discoverer 1.4 software (ThermoElectron Corp., San Jose, CA). Resulting DTA files from each data acquisition file were searched to identify CAT peptides against the custom databases using the MASCOT search engine (Matrix Science Ltd.; version 2.2.7; in-house licensed). Searches were done with non-specificity, allowing two missed cleavages, and a mass error tolerance of 7 ppm in MS spectra (i.e. FT-ICR data) and 0.7 Da for MS/MS ions. Identified peptides were generally accepted when the MASCOT ion score value exceeded 20. All the peptide assignments were also manually validated.